

# PREDISTORTION FOR POWER AMPLIFIER LINEARIZATION IN FULL-DUPLEX TRANSCEIVERS WITHOUT EXTRA RF CHAIN

Fernando H. Gregorio<sup>†</sup>, Gustavo J. González<sup>†</sup>, Juan Cousseau<sup>†</sup>, Taneli Riihonen<sup>‡</sup>, and Risto Wichman<sup>‡</sup>

<sup>†</sup>CONICET-Department of Electrical and Computer Engineering, Universidad Nacional del Sur, Argentina

<sup>‡</sup>Department of Signal Processing and Acoustics, Aalto University School of Electrical Engineering, Finland

## ABSTRACT

Genuine full-duplex operation requires effective mitigation of self-interference (SI) due to simultaneous transmission and reception at the same frequency band. In addition to its well-known harmful effect on signals of high peak-to-average power ratio, nonlinear behavior of a power amplifier (PA) complicates SI cancellation and induces spectral regrowth. We introduce a digital predistortion architecture that linearizes the response of the PA in a full-duplex transceiver. Specifically, we propose a two-step procedure to estimate the predistorter parameters and the SI canceller coefficients. Different from a direct application of conventional predistorters, the proposed architecture does not need an extra RF chain to estimate the PA response and exploits the inherent SI signal instead. Finally, simulation results show that the proposed scheme is able to increase significantly the signal-to-interference-plus-noise ratio at the transceiver output and to reduce out-of-band emissions when compared to linear and nonlinear cancellation without predistortion.

**Index Terms**— Full duplex, self-interference, nonlinear distortion, spectral regrowth, digital predistortion.

## 1. INTRODUCTION

Requirements of high data rates and network capacity over an increasingly saturated radio spectrum motivates full-duplex technology. The concept promises to increase the spectral efficiency by allowing simultaneous transmission and reception in the same band. Hence, data rate per allocated spectrum unit is ideally doubled w.r.t. conventional time- or frequency-division duplexing.

The implementation of the full-duplex mode is, however, challenging due to the strong self-interference (SI) produced by the transmitted signal that is coupled to the receiver front-end [1]. There are several options for removing the strong self-interference signal [2]. Usually passive/active antenna cancellation techniques together with RF canceller [3] are first employed to mitigate the SI at the input of the receiver chain and alleviate the requirements of the low-noise amplifier and the analog-to-digital converter (ADC). After that, an additional cancellation stage based on digital signal processing (DSP) is implemented to cope with residual interference [4, 5].

Linear, widely-linear and nonlinear DSP cancelers have already been studied for the residual SI cancellation. Specifically, nonlinear cancelers can remove nonlinear distortion effects generated by the transmitter PA and other imperfections of the transmitter chain [6, 7]. These techniques outperform basic linear cancellers in terms of in-band distortion cancellation, reaching isolation levels larger than 100 dB when combined with antenna and RF cancellation techniques.

Despite offering promising in-band performance, available solutions do not consider the out-of-band distortion generated by the PA nonlinearity. Even when the in-band distortion is removed by

a nonlinear canceler, the spectral regrowth increases when the PA is driven into power-efficient operation point. The resulting out-of-band emission reduces the spectral efficiency of full-duplex relays, because guard bands are needed to limit adjacent channel interference.

In this paper we introduce a predistorter (PD) to linearize the behaviour of the PA so that it can operate in its power-efficient region with moderate out-of-band distortion. While simplest PD structures are memoryless, such that the current output depends only on the current input [8], broadband implementations introduce memory effects that need to be considered: Volterra, Wiener, and Wiener-Hammerstein models as well as memory polynomials are generally used for these cases [9, 10]. Due to its generic modeling capabilities, we use here the Wiener-Hammerstein model to represent the behavior of the PA and the self-interference channel.

In contrast to previous full-duplex PD design [11], the proposed architecture does not need an extra RF chain to estimate the PA response and exploits the inherent SI signal instead. In particular, we propose a two-step procedure to estimate PD and SI parameters. First, using a low peak-to-average-power ratio training sequence, the linear part of the models related to the SI channel and the PA are estimated. Then, the PA nonlinearity is identified using a simple recursive algorithm. Besides significantly improving signal-to-interference-plus-noise ratio (SINR) at the relay output, our predistorter is also able to reduce the spectral regrowth and enhance the quality of the desired signal transmitted to a distant receiver.

## 2. SYSTEM MODEL

In this work, we consider a complete two-hop link composed of a source node, a full-duplex relay node and a destination node. The full-duplex mode allows the relay to receive and forward signals simultaneously in the same frequency band. Additionally, the relay performs non-regenerative processing such that each received orthogonal frequency-division multiplexing (OFDM) symbol is amplified and then retransmitted to the destination.

The received signal at the relay input is the following:

$$y_R(n) = h_{SR}(n) * x(n) + h_{SI}(n) * p(y_R(n - D)) + w_R(n) \quad (1)$$

where  $x(n)$  is the  $N$ -subcarrier OFDM signal from the source node,  $h_{SR}(n)$  is the source-relay channel,  $h_{SI}(n)$  models the loopback coupling channel,  $p(\cdot)$  defines the operation executed at the relay based on the input signal  $y_R(n - D)$  delayed by  $D$ -samples, and  $w_R(n)$  is white Gaussian noise. In case of the amplify-and-forward relay,

$$p(y_R(n - D)) = \beta y_R(n - D) \quad (2)$$

where  $\beta$  is a scalar gain.

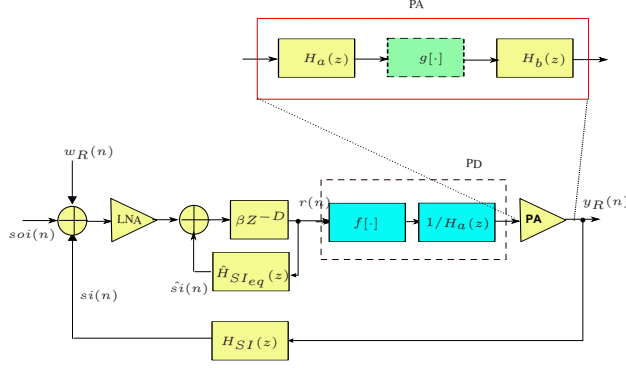


**Fig. 1.** Block diagram of full-duplex relay node with memory pre-distorter

At the destination, we have

$$y_D(n) = h_{RD}(n) * \beta y_R(n - D) + h_{SD}(n) * x(n) + w_D(n) \quad (3)$$

where  $h_{RD}(n)$  and  $h_{SD}(n)$  represent the relay-destination and source-destination channels, respectively, and  $w_D(n)$  denotes Gaussian noise at the receiver.

The self-interference term  $h_{SI}(n) * \beta y_R(n - \tau)$  needs to be mitigated to allow the relay to operate in FD mode. We assume that passive/active antenna cancellation and RF cancellation are included in this scenario such that,  $h_{SI}(n)$  denotes the residual channel before DSP cancellation.

### 3. IDENTIFICATION TECHNIQUE FOR SELF-INTERFERENCE CHANNEL AND PA PARAMETERS

We assume that the nonlinear amplifier is the dominant RF impairment. Thus, the down- and up-conversion processes, and the analog to digital conversion are assumed to be ideal.

#### 3.1. Nonlinear PA Model

PA response includes memory effects represented by a Wiener-Hammerstein (W-H) model. The Wiener-Hammerstein model consists of a cascade of a linear filter  $h_a(n)$ , and a nonlinear static function  $g[\cdot]$  followed by another linear filter  $h_b(n)$ . Herein,  $h_a(n)$  and  $h_b(n)$  are FIR filters of length  $L_a$  and  $L_b$ , respectively. The transmitted signal  $y_R(n)$  can now be expressed as

$$y_R(n) = \sum_{m=0}^{L_b} h_b(m) g[\tilde{r}(n - m)] \quad (4)$$

where  $\tilde{r}(n) = \sum_{m=0}^{L_a} h_a(m) r(n - m)$ .

The static non-linearity is modeled as a  $P$ -th order polynomial with coefficients  $\{g_{2k+1}\}_{k=0}^K$ , described by

$$g[s(n)] = \sum_{k=0}^K g_{2k+1} \phi_{2k+1}[\tilde{r}(n)] \quad (5)$$

where  $\phi_{2k+1}[\tilde{r}(n)] = \tilde{r}(n) |\tilde{r}(n)|^{2k}$  with

$$2k + 1 = \begin{cases} P & P \text{ even} \\ P - 1 & P \text{ odd} \end{cases}$$

#### 3.2. Proposed Identification Technique

In this subsection, an identification technique of PA parameters and self-interference channel is proposed. Specifically, the required parameters to implement the PD and SI canceller, as illustrated in Fig. 1 are:

- Equivalent self-interference channel: the channel estimate is employed by the DSP canceller to remove the self-interference signal. It is composed by the cascade of  $H_b(z)$ ,  $H_{SI}(z)$ , and the LNA.
- Power amplifier model: the estimates of  $H_a(z)$  and the inverse of nonlinear block  $g[\cdot]$ , denoted by  $f[\cdot]$ , are used to implement a PD that linearizes the PA.

The required parameters are estimated during a short initialization period operating in a half-duplex manner. The wireless channel and PA parameters are assumed to be time-invariant so that they need not be tracked.

A two-step procedure for the identification is proposed. The first step employs a training sequence with low PAPR that allows to estimate the linear cascade of  $H_a(z)$ ,  $H_b(z)$ , and  $H_{SI}(z)$  without the influence of the nonlinear static block  $g[\cdot]$ . Then in the second step, the static nonlinearity  $f[\cdot]$  and the linear filter  $H_a(z)$  are identified.

##### 3.2.1. Estimation of the linear equalizer coefficients (Step 1)

To obtain a reliable estimate of the linear cascade it is important that training symbols are not affected by the nonlinearity  $g[\cdot]$ . By using a low PAPR sequence, generated by using a set of  $T$  active subcarriers, where  $T < N$ , the PA mostly operates in the linear region. In this case, the received signal can be written as:

$$y(n) = h_a(n) \circledast h_b(n) \circledast h_{si}(n) \circledast x_T(n) + w_R(n) \quad (6)$$

where  $\circledast$  is the circular convolution and  $x_T(n)$  is the training sequence.

A block diagram of the linear cascade estimation block is shown in Fig. 2. The objective is to design an equalizer, denoted by  $\Psi$ , that compensates for the memory-channel effects in order to get  $y_{eq}(n)$ . To this end, we define a  $1 \times L_z$  equalizer vector  $\Psi = [\psi(0), \psi(1), \dots, \psi(L_z - 1)]$ .

After the equalization, the output can be written as

$$y_{eq}(n) = \Psi \mathbf{y}(n) \quad (7)$$

where  $\mathbf{y}(n) = [y(n), y(n-1), \dots, y(n-L_z)]^T$  is the received signal. Equalizer coefficients are calculated using the least-squares (LS) criterion as

$$\Psi = (\mathbf{Y}^H \mathbf{Y})^{-1} \mathbf{Y}^H \mathbf{x}_T \quad (8)$$

where  $\mathbf{Y}$  is a  $L \times L_z$  matrix

$$\mathbf{Y} = [\mathbf{y}(0), \mathbf{y}(1), \dots, \mathbf{y}(L-1)] \quad (9)$$

$\mathbf{x}_T = [x_T(0), x_T(1), \dots, x_T(L-1)]^T$  is the training sequence, and  $L$  is the number of samples employed for equalizer estimation (training sequence length). Instead of LS estimate, it is possible to use a recursive least-squares (RLS) algorithm or some conventional frequency domain channel estimation technique.

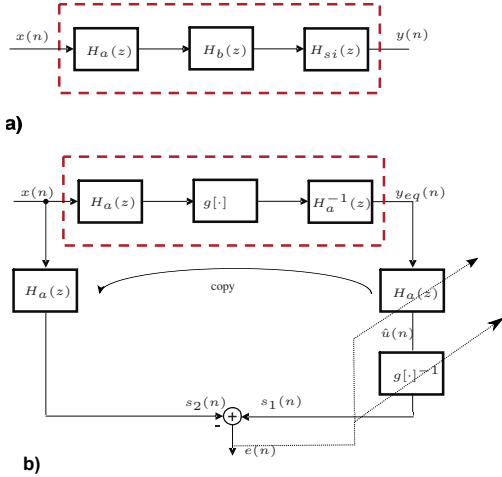


**Fig. 2.** a) Linear cascade identification (Step 1) and b) nonlinear block identification (Step 2).

### 3.2.2. Estimation of the NL block (Step 2)

In order to estimate the nonlinear block, a normal OFDM sequence that excites the PA in its complete dynamic range is employed. In the absence of noise and assuming perfect equalization, the two sequences  $x(n)$  and  $y_{eq}(n)$  are related as follows

$$\begin{aligned} y_{eq}(n) &= g[x(n) \otimes h_a(n)] \otimes h_b(n) \otimes h_{s1}(n) \otimes \psi(n) \\ &= g[x(n) \otimes h_a(n)] \otimes \{h_a\}^{-1}(n) \end{aligned} \quad (10)$$

where  $\{h_a\}^{-1}(n)$  denotes the inverse of the filter  $h_a(n)$ . This observation allows to estimate  $H_a(z)$  and  $g^{-1}[\cdot]$  using the structure in Figure 2 b) [12]. The proposed algorithm minimizes the error  $e(n) = \hat{s}_1(n) - \hat{s}_2(n)$  between

$$\begin{aligned} \hat{s}_1(n) &= \sum_{k=0}^P f_{2k+1}(n) \phi_{2k+1}[\hat{u}(n)] \\ \hat{s}_2(n) &= \hat{\mathbf{h}}_a^H \mathbf{x}(n) \end{aligned} \quad (11)$$

where  $f[\cdot]$  is the  $p$ -th order inverse of the static nonlinearity  $g[\cdot]$ , the vector  $\hat{\mathbf{h}}_a$  is defined as  $\hat{\mathbf{h}}_a = [\hat{h}_a(0), \hat{h}_a(1), \dots, \hat{h}_a(L_a - 1)]$  and the input vector is given by  $\mathbf{x}(n) = [x(n), x(n-1), \dots, x(n-L_a)]^T$ . The intermediate variable  $\hat{u}(n)$  is given by:

$$\hat{u}(n) = \hat{\mathbf{h}}_a [y_{eq}(n), y_{eq}(n-1), \dots, y_{eq}(n-L_a)]^T \quad (12)$$

To avoid ambiguity in the filter gain [13],  $\hat{h}_a(0)$  is anchored to a fixed value. The error to be minimized can be written as

$$e(n) = \hat{s}_1(n) - \hat{s}_2(n) = \theta^H(n) \varphi(n) - \hat{h}_a(0)^* x(n) \quad (13)$$

where vectors  $\theta(n) \in \mathbb{C}^{(P+L_a+1) \times 1}$  and  $\varphi(n) \in \mathbb{C}^{(P+L_a+1) \times 1}$  are given by

$$\begin{aligned} \theta(n) &= [\mathbf{f}^T(n), \hat{\mathbf{h}}_a^T(n)]^T \\ \varphi(n) &= [\phi[\hat{u}(n)]^T, -\mathbf{x}^T(n)]^T \end{aligned} \quad (14)$$

and

$$\mathbf{f}(n) = [f_1(n) f_3(n) \dots f_{2P+1}(n)]^T$$

$$\hat{\mathbf{h}}_a(n) = [\hat{h}_{a1}(n) \hat{h}_{a2}(n) \dots, \hat{h}_{aL_a}(n)]^T \quad (15)$$

$$\phi[\hat{u}(n)] = [\phi_1[\hat{u}(n)] \phi_3[\hat{u}(n)] \dots, \phi_{2P+1}[\hat{u}(n)]]^T$$

Using the instantaneous squared error  $|e(n)|^2$  as an objective function, a stochastic gradient algorithm that updates  $\theta(n)$  is given by

$$\theta(n+1) = \theta(n) - \mu e^*(n) \nabla_{\theta} [e(n)] \quad (16)$$

where  $\mu$  is a step size controlling the convergence speed and algorithm stability. The gradient in (16) is given by

$$\nabla_{\theta} [e(n)] = \begin{bmatrix} \nabla_{\mathbf{f}} [s_1(n)] \\ \nabla_{\hat{\mathbf{a}}} [s_1(n)] - \nabla_{\hat{\mathbf{a}}} [s_2(n)] \end{bmatrix} \quad (17)$$

where

$$\nabla_{\mathbf{f}} [s_1(n)] = \phi[\hat{u}(n)]$$

$$\nabla_{\hat{\mathbf{a}}} [s_2(n)] = \mathbf{x}(n)$$

$$\begin{aligned} \nabla_{\hat{\mathbf{a}}} [s_1(n)] &= \left( f_1(n) + \sum_{k=0}^{P-1} (2k+3) f_{2k+3}(n) \phi_{2k+1}[\hat{u}(n)] \right) \\ &\quad \times \mathbf{y}_{eq}(n) \end{aligned} \quad (18)$$

and  $\mathbf{y}_{eq}(n) = [y_{eq}(n), y_{eq}(n-1), \dots, y_{eq}(n-L_a)]^T$ . Verification of  $\nabla_{\hat{\mathbf{a}}} [s_1(n)]$  in (18) is straightforward, and is presented in the following:

Using (14) and (15), it is possible to obtain

$$\nabla_{\hat{\mathbf{a}}} [s_1(n)] = \frac{\partial s_1(n)}{\partial \hat{u}(n)} \frac{\partial \hat{u}(n)}{\partial \hat{\mathbf{a}}(n)} = \frac{\partial s_1(n)}{\partial \hat{u}(n)} \mathbf{y}_{eq}(n) \quad (19)$$

To proceed we need to employ the basic passband representation of the conventional polynomial model, i.e.,

$$\tilde{s}_1(n) = \sum_{k=0}^P \tilde{f}_k \tilde{u}^k(n) \quad (20)$$

where  $\tilde{(\cdot)}$  is the notation for passband signal and coefficients and  $P$  is the order of the polynomial model. To obtain  $\frac{\partial s_1(n)}{\partial u(n)}$ , avoiding the problem of baseband model differentiation, we can first differentiate (20) with respect to  $\tilde{u}(n)$  and then transform the result to baseband. The differentiation in passband is straightforward and is given by

$$\frac{\partial \tilde{s}_1(n)}{\partial \tilde{u}(n)} = \sum_{k=1}^P k \tilde{f}_k \tilde{u}^{k-1}(n) \quad (21)$$

where  $\tilde{f}'_k = k \tilde{f}_k$ . The baseband form of (21) is given by [14] (considering  $u(n)$  as a narrowband signal)

$$\begin{aligned} \frac{\partial s_1(n)}{\partial u(n)} &= f_1 + \sum_{k=0}^{P-1} f'_{2k+3} [u^{k+1}(n) (u^*(n))^k] \\ &= f_1 + \sum_{k=0}^{P-1} (2k+3) f_{2k+3} |u(n)|^{2k} u(n) \end{aligned} \quad (22)$$

Except for the constant  $f_1$  and the order of the polynomial, the derivative has the same form as the memoryless polynomial model.

**Table 1.** Adjacent channel power leakage ratio (ACLR) for different PA back-off levels; the values are calculated for an operation band of 10 MHz when the first adjacent band is at 7–12 MHz.

PA IBO	ACLR with LC	ACLR with NLC	ACLR with PD+LC
-2 dB	-30.4 dB	-34.0 dB	-41.0 dB
-4 dB	-33.5 dB	-38.4 dB	-45.9 dB
-6 dB	-37.3 dB	-42.9 dB	-46.5 dB

### 3.3. Implementation of Predistorter and SI Canceller

◇ **PD and linear canceller:** From the identification algorithm developed in the previous section we obtain: a) the PD coefficients, b) the linear cascade estimate of  $H_a(z)$ ,  $H_b(z)$ , and  $H_{SI}(z)$ , and c) the estimate of  $H_a(z)$ . A Wiener PD is implemented by using the nonlinear PD coefficients and the estimate of  $H_a^{-1}(z)$ . A linear canceller is implemented using the estimate  $\hat{H}_{SI_{eq}}$  that is formed by the SI channel and the linear filter placed after the nonlinear block, i.e.,  $H_{SI}(z)H_b(z)$ . A block diagram of full duplex relay including PD and DSP canceller is illustrated in Fig. 1.

◇ **Nonlinear canceller:** The NLC takes into account the nonlinear distortion produced by the nonlinear PA. The estimate of the SI signal can be expressed as

$$\hat{s}_{NLC}(n) = \hat{g}[r(n) * \hat{h}_a(n)] * \hat{h}_{SI_{eq}}(n)G_{LNA} \quad (23)$$

where  $r(n)$  is the digital baseband signal obtained before the PA,  $G_{LNA}$  is the low-noise amplifier gain, and  $\hat{g}[\cdot]$ ,  $\hat{h}_{SI_{eq}}(n)$ , and  $\hat{h}_a(n)$  are the estimates of the PA response, the equivalent SI channel and the linear filter  $h_a(n)$  respectively.

◇ **Linear canceller:** The LC assumes a linear a PA. The estimate of the SI signal is given by

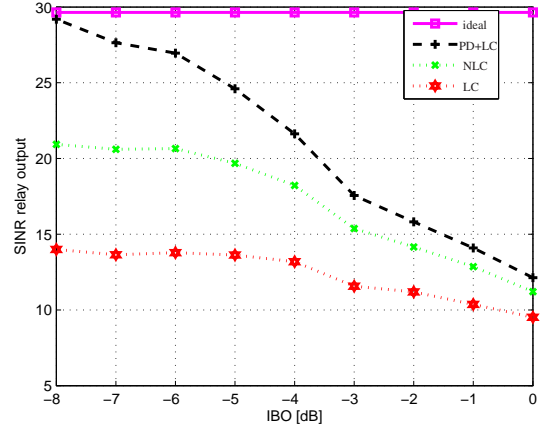
$$\hat{s}_{LC}(n) = r(n) * \hat{h}_a(n) * \hat{h}_{SI_{eq}}(n)G_{LNA}. \quad (24)$$

## 4. SIMULATION RESULTS AND CONCLUSIONS

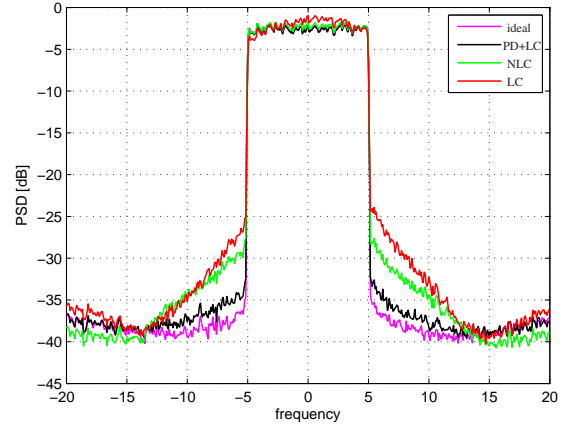
A full-duplex relay scenario is evaluated assuming OFDM transmission with  $N = 512$  subcarriers and 10 MHz system bandwidth. Transmit power is 0 dBm, and passive/antenna cancellation and RF cancellation with 50 dB and 30 dB attenuation, respectively, are assumed. The SNR at the relay node is 30 dB. The self-interference channel is modeled as a FIR filter, where the main path and multipath components have a power difference, K-factor, of 30 dB. At initialization, one OFDM symbol with  $T = 32$  active subcarriers is used to identify the linear cascade and 20 OFDM symbols are required to identify the NL block. The predistorter was implemented using a polynomial with  $P = 7$  (only odd terms) and the linear block was identified using  $L_a = 5$  coefficients. The results are averaged over 100 SI channel and noise realization, and 8-time oversampling is used to evaluate the spectral regrowth. The power amplifier is modeled as a W-H system, where the linear filters are given by [15]

$$H_a(z) = \frac{1 + 0.1z^{-2}}{1 - 0.1z^{-1}} \quad \text{and} \quad H_b(z) = \frac{1 - 0.1z^{-1}}{1 - 0.2z^{-1}}, \quad (25)$$

and the static nonlinearity follows a solid state power amplifier (SSPA) response employing the Saleh model with smoothing factor  $p = 2$  and clipping level  $C_L = 1$ . The PA operation point is controlled using a backoff, that is defined as  $IBO = 10 \log_{10} \frac{P_{i_{sat}}}{P_i}$ , where  $P_{i_{sat}}$  is the input saturation power and  $P_i$  is the input power.



(a) In-band distortion when the PA operates with different IBOs



(b) Out-of-band distortion when PA operates with an IBO of -4 dB

**Fig. 3.** The effect of distortion at relay output with a linear DSP canceller, nonlinear canceller and predistorter.

The signal-to-interference-and-noise ratio (SINR) at the output of the node relay is employed to quantify the relay performance. It includes the channel noise, residual SI and PA distortion. Figure 3(a) illustrates the SINR at the output obtained for the PA operating with different IBO. The curves show the advantage of using the predistorter (PD) with linear canceller compared with nonlinear canceller (NLC) and linear canceller (LC) techniques. The PD outperforms NLC and LC techniques in terms of SINR for severe PA distortion. The performance in terms of the out-of-band distortion is shown in Fig. 3(b). The figure depicts the power spectral density (PSD) at the relay output verifying the advantage of the PD technique. Table 1 illustrates adjacent channel leakage in the same cases.

In summary, the obtained results show that the proposed scheme is able to increase significantly the signal-to-interference-plus-noise ratio at the transceiver output and to reduce out-of-band emissions in comparison to linear and nonlinear cancellation without predistortion. Moreover, the quality of the desired signal transmitted to a distant receiver is also improved with predistortion, while mere nonlinear cancellation does not reduce the effects of PA nonlinearities in the transmitted signal.

## 5. REFERENCES

- [1] M. Duarte, C. Dick, and A. Sabharwal, "Experiment-driven characterization of full-duplex wireless systems," *IEEE Trans. Wireless Commun.*, vol. 11, no. 12, pp. 4296–4307, Dec. 2012.
- [2] M. Heino, D. Korpi, T. Huusari, E. Antonio-Rodríguez, S. Venkatasubramanian, T. Riihonen, L. Anttila, C. Icheln, K. Haneda, R. Wichman, and M. Valkama, "Recent advances in antenna design and interference cancellation algorithms for in-band full duplex relays," *IEEE Communications Magazine*, vol. 53, no. 5, pp. 91–101, May 2015.
- [3] K. E. Kolodziej, J. G. McMichael, and B. T. Perry, "Multi-tap RF canceller for in-band full-duplex wireless communications," *IEEE Trans. Wireless Commun.*, vol. 15, no. 6, pp. 4321–4334, Jun. 2016.
- [4] A. Raghavan, E. Gebara, E. M. Tentzeris, and J. Laskar, "Analysis and design of an interference canceller for collocated radios," *IEEE Trans. Microw. Theory Tech.*, vol. 53, no. 11, pp. 3498–3508, Nov. 2005.
- [5] D. Korpi, T. Huusari, Y.-S. Choi, L. Anttila, S. Talwar, and M. Valkama, "Digital self-interference cancellation under non-ideal RF components: Advanced algorithms and measured performance," in *Proc. IEEE 16th International Workshop on Signal Processing Advances in Wireless Communications (SPAWC)*, June 2015, pp. 286–290.
- [6] D. Korpi, Y.-S. Choi, T. Huusari, L. Anttila, S. Talwar, and M. Valkama, "Adaptive nonlinear digital self-interference cancellation for mobile inband full-duplex radio: Algorithms and RF measurements," in *Proc. IEEE Global Communications Conference (GLOBECOM)*, Dec. 2015, pp. 1–7.
- [7] E. Ahmed, A. M. Eltawil, and A. Sabharwal, "Self-interference cancellation with nonlinear distortion suppression for full-duplex systems," in *Proc. Asilomar Conference on Signals, Systems and Computers*, Nov. 2013, pp. 1199–1203.
- [8] C. Eun and E. J. Powers, "A new Volterra predistorter based on the indirect learning architecture," *IEEE Trans. Signal Process.*, vol. 45, no. 1, pp. 223–227, Jan. 1997.
- [9] L. Ding, G. T. Zhou, D. R. Morgan, Z. Ma, J. S. Kenney, J. Kim, and C. R. Giardina, "A robust digital baseband predistorter constructed using memory polynomials," *IEEE Trans. Commun.*, vol. 52, no. 1, pp. 159–165, Jan. 2004.
- [10] P. Gilibert, G. Montoro, and E. Bertran, "On the Wiener and Hammerstein models for power amplifier predistortion," in *Proc. Asia-Pacific Microwave Conference (APMC)*, Dec. 2005.
- [11] A. C. M. Austin, A. Balatsoukas-Stimming, and A. Burg, "Digital predistortion of power amplifier non-linearities for full-duplex transceivers," in *IEEE 17th International Workshop on Signal Processing Advances in Wireless Communications (SPAWC)*, July 2016.
- [12] A. D. Kalafatis, L. Wang, and W. R. Cluett, "Identification of Wiener-type nonlinear systems in noisy environment," *Int. J. Control*, vol. 66, pp. 923–941, Apr. 1997.
- [13] N. Bershad, S. Bouchired, and F. Castanie, "Stochastic analysis of adaptive gradient identification of Wiener-Hammerstein systems for Gaussian inputs," *IEEE Trans. Signal Process.*, vol. 48, no. 2, pp. 557–560, Feb. 2000.
- [14] S. Benedetto, E. Biglieri, and R. Daffara, "Modeling and performance evaluation of nonlinear satellite links — A Volterra series approach," *IEEE Trans. Aerospace Elec. Syst.*, vol. AES-15, no. 4, pp. 494–507, Jul. 1979.
- [15] R. Raich, H. Qian, and G. T. Zhou, "Orthogonal polynomials for power amplifier modeling and predistorter design," *IEEE Trans. Veh. Technol.*, vol. 53, no. 5, pp. 1468–1479, Sep. 2004.